PFG 2013 / 6, 0551 – 0562
Stuttgart, December 2013

Article

UAV-based Imaging for Multi-Temporal, very high Resolution Crop Surface Models to monitor Crop Growth Variability

Juliane Bendig, Andreas Bolten & Georg Bareth, Köln

Keywords: agriculture, crop growth, DEM, plant height, UAV

Summary: This paper describes the generation of multi-temporal crop surface models (CSMs) with very high resolution of < 0.05 m. Data collection was carried out with a low-cost and low-weight UAV-system with a weight of less than 5 kg and the possibility of mounting different sensors. Key focus is the detection of crop growth variability and its dependency on cultivar, crop treatment and stress. The study area is a barley experiment field in Bonn in the west of Germany. Four replications of four cultivars of barley were investigated of which half of them where treated with a fungicide. Five UAV-campaigns were carried out during the growing season between early May and late July 2012. Ground control points (GCPs) measured with a HiPer Pro Topcon DGPS allowed for appropriate ground truth (< 0.02 m). Ground based infield control surveys on three dates served as validation of the method. Additionally, various destructive and non-destructive ground data were collected. The stereo images captured were processed into CSMs by using the structure-from-motion (SfM) software Agisoft PhotoScan. Generated plant heights ranged between 0.16 m and 0.983 m. R^2 (n = 32) for the correlation between plant heights in the CSM and infield control surveys is 0.69. Lower plant heights were detected in those plots of the field where no fungicide was applied. Height differences between cultivars were observed and increased during growing season. The accuracy assessment of DEMs generated with the proposed UAV-based imaging showed a correlation coefficient of 0.99 (n = 10) between the DGPS GCPs and the DEMs with a mean difference of 0.01 m in z-direction.

Zusammenfassung: *Monitoring des Pflanzenwachstums mit Hilfe multitemporaler und hoch auflösender Oberflächenmodelle von Getreidebeständen auf Basis von Bildern aus UAV-Befliegungen.* Dieser Beitrag beschreibt die Erzeugung von multitemporalen Oberflächenmodellen von Getreidebeständen (crop surface models, CSMs) mit einer sehr hohen Auflösung von < 0.05 m. Die Datenerfassung wurde mit einem kostengünstigen UAV-System mit einem Gewicht von weniger als 5 kg durchgeführt, welches die Möglichkeit der Anbringung verschiedener Sensoren bietet. Schwerpunkt war die Detektion der Variabilität im Pflanzenwachstum und die Abhängigkeit von Sorte, Pflanzenbehandlung und Stress. Das Untersuchungsgebiet liegt in Bonn im Westen Deutschlands und besteht aus 32 Testflächen, die mit viermaliger Wiederholung mit je vier Gerstensorten bepflanzt wurden, Die Hälfte der Pflanzen wurde mit einem Fungizid behandelt. Die Untersuchung umfasste fünf UAV-Kampagnen während der Vegetationsperiode zwischen Anfang Mai und Ende Juli 2012. Passpunkte (GCPs), gemessen mit einem HiPer Pro Topcon DGPS, sorgten für eine entsprechende Georeferenzierung (< 0.02 m). Kontrollmessungen im Feld an drei Terminen dienten zur Validierung der Methode. Zusätzlich wurden weitere destruktive und nicht-destruktive Felddaten erhoben. Aus den Stereobildern wurden unter Verwendung der Structure-from-Motion (SfM) Software Agisoft PhotoScan CSMs erzeugt. Die abgeleiteten Pflanzenhöhen lagen zwischen 0,16 m und 0,983 m. Das R^2 für die Korrelation zwischen Pflanzenhöhe im CSM und den Kontrollmessungen liegt bei 0,69. Niedrigere Pflanzenhöhen befanden sich in ungespritzten Teilen des Feldes. Höhenunterschiede zwischen den Sorten wurden festgestellt, die sich während der Vegetationsperiode verstärkten. Die Genauigkeitsanalyse des UAV-basierten DEMs zeigte einen Korrelationskoeffizienten von 0,99 zwischen DGPS und DEM, mit einer mittleren Differenz von 0,01 m in Z-Richtung.

www.schweizerbart.de
DOI: 10.1127/1432-8364/2013/0200
1432-8364/13/0200 $ 3.00

1 Introduction

Modelling canopy surfaces is a common application of remote sensing methods. In forestry, stereo photogrammetry or airborne laser scanning (ALS) are used for the extraction of canopy heights and surface modelling (St-Onge et al. 2008). Spaceborne sensors like TerraSAR-X combined with TanDEM-X enable stereo radargrammetric modelling of canopy heights (Perko et al. 2010).

Precision agriculture can benefit greatly from remote sensing (Mulla 2012). Small experiment fields (< 5 ha) like the one presented in this study can be easily monitored using low-weight unmanned aerial vehicles (UAVs). Producing multi-temporal datasets of the whole vegetation period is essential for obtaining reliable results in such experiments.

UAVs are already in use for capturing optical, spectral and thermal information (Eisenbeiss & Sauerbier 2011, Grenzdörffer et al. 2008, Hunt et al. 2010, Hartmann et al. 2012).

The UAV-system used in this study is a low-cost multi-sensor system with a weight of less than 5 kg, a so called Mini-UAV (Eisenbeiss 2009). Using a high resolution RGB consumer camera, stereo images can be captured and processed into digital crop surface models (CSMs) (Fig. 1).

The key focus is to detect differences in plant height depending on cultivar, phenology, crop treatment, or stress. The non-invasive measurement of plant height is important due to its correlation to biomass and other crop parameters (Hansen & Schjoerring 2003, Thenkabail et al. 2000). In this context, Hoffmeister et al. (2010) introduced the concept of multi-temporal CSMs for monitoring plant growth between phenological stages with terrestrial laserscanning. Comparison of the CSMs for different phenological stages allows for the detection of crop growth variability and absolute plant height. This approach of analysing CSMs is shown in Fig. 1. The plant height (PH), e.g. at time t_3 results from t_3 minus t_0. The plant growth (PG), for example from time t_1 to time t_3 results from t_3 minus t_1.

In this study, the idea of investigating multi-temporal CSMs is transferred to very high resolution CSMs derived from stereo images captured by a UAV.

2 Data Acquisition

2.1 *Study Area and Dataset*

The study area is located in the city of Bonn in the west of Germany (Fig. 2). In 2012 the *Institute for Agricultural Plants and Resource Protection* (INRES*) – Horticultural Science* established an experiment field with four different cultivars of barley with different resistances to plant diseases.

The aim of the experiment is to determine the response to natural pathogens using non-

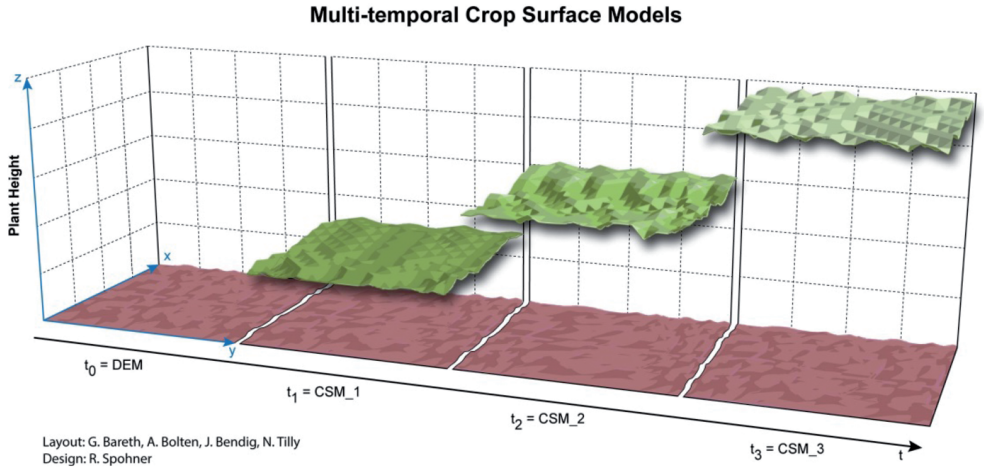

Fig. 1: Multi-temporal crop surface models (CSMs).

destructive measurement techniques. A protective and curative fungicide against three common plant diseases was applied to the control sample plants (grey plots in Fig. 2). All other horticultural activities were left unchanged. Four replications of every cultivar for both treatments were planted in 1.5 m x 7 m plots in a randomised order surrounded by boundary plots which were not used for measurements.

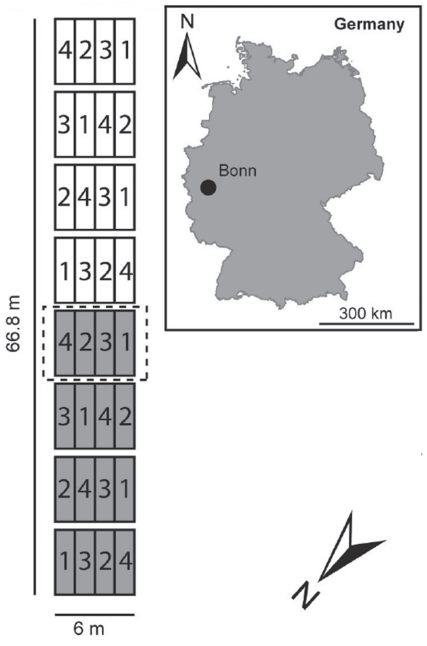

Fig. 2: Study area – 4 replications of 4 cultivars of barley (1, 2, 3, 4) planted in randomised order, two treatments. Grey: treated plots, white: untreated plots, dashed line: replication 4 (treated).

Fig. 3: MK-Oktokopter by HiSystems GmbH mounted with RGB sensor.

The ground based data collection was seperated into destructive sampling of biomass, plant N- and chlorophyll content, and non-destructive data acquisition of plant height, hyperspectral, and fluorescence data. Field data campaigns were carried out repeatedly during the growing season. UAV campaigns were conducted on 14.5., 25.5., 5.6, 18.6. and 23.7.12 using an RGB sensor (see section 2.3). 18 ground control points (GCPs) were established on the corners of the plots for ground truth. Infield control surveys of the plant heights were carried out on the 25.5., 5.6. and 18.6.12.

2.2 *Platform*

The UAV-system is a MK-Oktokopter by HiSystems GmbH (HiSystems GmbH 2013). It consists of a point-symmetrical frameset composed of aluminium and glass fibre reinforced plastics (Fig. 3). The total weight of the system including battery is less than 2.5 kg. An additional payload of up to 1 kg is possible. The cost of the entire system not including the sensor is around 3,000 €. The eight engines are equipped with high performance propellers.

The electronics include high-quality gyroscopes, a pressure sensor, a compass module and a GPS module (Mikrokopter 2013a). Using the open source software Mikrokopter-Tool (Mikrokopter 2013b) pre-defined flight routes in a sense of an auto-pilot can be carried out in autonomous flight mode. Lithium polymer batteries with up to 6,600 mAh capacity enable flight times of around 15 minutes depending on the payload. The additional transmitter channels of the 2.4 GHz transmitter remote control are used for camera triggering (Bendig et al. 2012).

2.3 *Sensor*

The RGB sensor is a Panasonic Lumix DMC GF3 with a Lumix G 20 mm (F1.7 ASPH) lens. The weight is 400 g and the sensor resolution is 4016 x 3016 (12 million) pixel (Panasonic 2013).

The field of view (FOV) of the camera is 48.5° horizontal and 33.4° vertical resulting in an image size of 90 m x 60 m at a distance of

100 m. Aperture and exposure times are adjusted and fixed manually prior to each flight. Due to the manual triggering of the camera an individually adapted camera holder with a mechanical trigger is used and operated by the remote control of the UAV-system.

2.4 *Data Acquisition*

Wooden poles with 0.3 m x 0.3 m highly visible targets attached to them were used as GCPs. Those were measured using a HiPer Pro Topcon DGPS with a horizontal and vertical accuracy of < 0.01 m according to own evaluations (0.02 m according to Ascos PED 2010). Horizontal coordinates of eight data acquisition points were taken in the field which were used as waypoints for the flight route, resulting in a 50% overlap of the images, covering the whole experimental field in one flight. Several flights were carried out for each field campaign with the sensor mounted in nadir position with constant orientation and flying height. For the Panasonic Lumix DMC GF3 a height of 30 m was chosen resulting in a FOV of 18 m x 27 m and ground resolution of 0.006 m.

For the infield control surveys a ruler was placed next to the plants on three positions in each of the 32 plots to determine the mean plant height per plot with a 0.01 m precision. Plant heights per plot vary 0.1 m on an average.

2.5 *Data Processing*

The overall workflow of data processing is presented in Fig. 4. For the generation of the CSM the multi-view 3D reconstruction software Agisoft PhotoScan 0.9.0 (Agisoft 2013) was used which is based on a structure-from-motion (SfM) algorithm (Verhoeven 2011). SfM allows for the estimation of the unknown camera positions through comparison of detected image feature points, e. g. object edges, in multiple images (Szeliski 2010). Despite of the fact that Agisoft PhotoScan and, in general, the use of SfM algorithms for DEMs derived from UAV-based imagery is becoming more and more popular since 2012, quite little literature on comparable studies has been published. Papers by Neitzel & Klonowski (2011), Verhoeven et al. (2012) and De Reu et al. (2013) suggest that the software shall be well suited for such applications.

For each date (except 23.7.) two partly overlapping tiles were generated, one covering the treated plots of the experiment field and one covering the untreated plots. However, a complete model could be generated as well. Due to computation and calculation time, we split the model into two parts. The point clouds con-

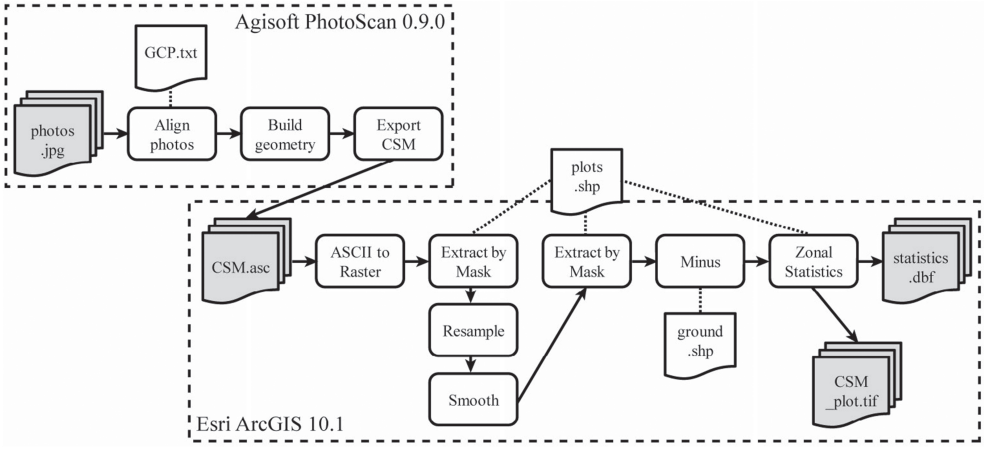

Fig. 4: Data Processing workflow for the generation of CSM (CSM.asc) from RGB images captured by UAV (photos.jpg) in Agisoft PhotoScan and further processing for analysis based on each plot in Esri ArcGIS.

sisted of 12 million points per model on average. As a result, the 4th replication of the untreated plots was covered in both datasets (Fig. 5).

GCPs were identified manually on each photo and assigned to the coordinates measured by the DGPS (Fig. 4). In a batch process the images were aligned to each other, the CSM was built.

Via an ASCII-file it was transferred to a raster file in Esri ArcGIS 10.1. A shapefile containing the outlines of the plots, reduced by a 0.3 m inside buffer to reduce plot boundary effects, served as a mask to extract areas of interest (AOI). After that, data were resampled to a raster size of 0.1 m and smoothed by calculating the focal mean of 3 x 3 pixel rectangles. A ground model was constructed from z-data of the GCPs (t_0 in Fig. 1). Each CSM was subtracted from the ground plane using the AOI shapefile to obtain plant height per plot. In a last step, general statistics including mean plant height and standard deviation were calculated for each date and plot.

Five datasets were collected during the growing season of which four could be used for analysis. For t_5 (23.7.), the CSM could only be generated for parts of the experiment field due to image quality (see Tab. 1). Image quality was decreased because of strong wind during data collection and lodging caused by a thunderstorm a few days before. Furthermore, parts of the CSM for t_3 (16.5.) and t_4 (18.6.) could not be modelled satisfactorily (t_3: replications 1–4 treated, replication 2 untreated; t_4: replication 4 treated, replication 3 and 1 untreated) resulting in unrealistic values for plant height. Those datasets were partly excluded from the analysis and are referred to as "selected data" in the following (Tab. 2, Fig. 7). Results of the analysis are presented for all data and selected data of sufficient quality.

3 Results

3.1 *Statistics*

Tab. 1 illustrates minimum, maximum, range, mean, and standard deviation (std.) of plant height for the whole experimental field according to date (t) and measurement technique (CSM or infield control survey). Plant heights generated from CSMs range from 0.16 m to 0.983 m over all dates. Ranges for

Tab. 1: Descriptive statistics of plant heights (m) derived from CSMs and infield control survey according to date (std. = standard deviation, RMSE = root-mean-square error).

	date	t_1	t_2	t_3	t_4	t_5
		14.5.12	25.5.12	5.6.12	18.6.12	23.7.12
CSM	min	0.160	0.354	0.595	0.454	0.228
	max	0.309	0.512	0.905	0.874	0.983
	range	0.149	0.158	0.310	0.420	0.755
	mean	0.241	0.451	0.772	0.688	0.595
	std.	0.028	0.032	0.062	0.075	0.160
	RMSE	0.256	0.453	0.815	0.683	0.892
infield control survey	min	no data	0.370	0.685	0.850	no data
	max		0.590	0.855	1.060	
	range		0.220	0.170	0.210	
	mean		0.509	0.763	0.950	
	std.		0.054	0.045	0.058	
	RMSE		0.702	0.755	0.940	

each date vary between 0.149 m and 0.755 m and increase with development of vegetation (range (t_5) > range (t_1)). The mean plant height increases for t_1 to t_3 and decreases for t_4 to t_5. Standard deviation increases continuously with the vegetation development (std. (t_5) > std. (t_1)). For the infield control surveys, plant heights range between 0.370 m and 1.06 m for all dates (t_2 to t_4). Ranges for each date vary between 0.17 m and 0.22 m which is significantly lower compared to the CSM heights. Mean plant height increases from t_2 to t_4 while the standard deviation varies without a trend.

The average difference of mean plant height between CSM and infield control survey is under 0.01 m for t_2 and t_3 but one magnitude higher for t_4. R^2 (correlation, n = 32) for both measurement techniques are 0.55 (t_2), 0.22 (t_3) and 0.71 (t_4). The overall correlation is 0.69 (n = 96) for the three dates altogether. For selected data, overall correlation decreases to 0.62 (n = 64), because some values were removed (R^2 t_3 = 0.43 (n = 12), R^2 t_4 = 0.68 (n = 20)).

3.2 *Crop Surface Models*

In Fig. 5 an example of the generated CSM with 0.006 m resolution is presented for t_2 (25.5.) starting with replication 1 (treated) in the north. The experiment plots, e. g. red rectangle in Fig. 5, are surrounded by two boundary plots on one side and three on the other side.

The plots can be clearly distinguished from each other and from the surrounding bare soil. Since the model was separated into two tiles, seamlines are visible. Tiles were not merged in order to keep the original data and to facilitate the comparison between the datasets. A closer look at replication 4 (treated) for t_0 to t_3 (Fig. 6) allows for the detection of possible differences in the datasets. Blue surfaces show plant height for t_1 (14.5.). An increasing height difference to the south (mean: 0.08 m, max: 0.18 m) is noticeable. For t_2 (25.5.), green surfaces in Fig. 6, the maximum difference is considerably lower with 0.11 m and the mean

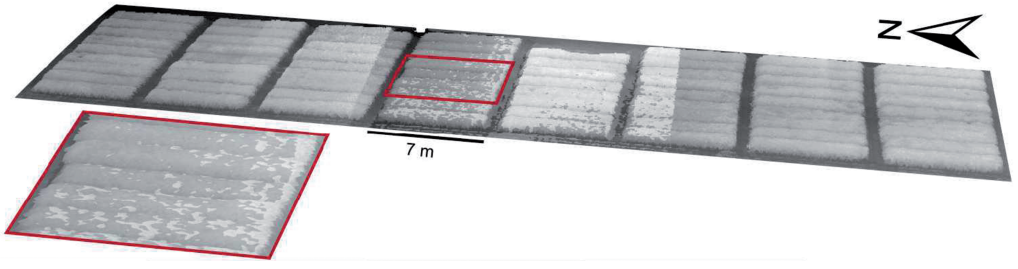

Fig. 5: CSM – Overview of study area (t_2: 25.5.2012), red rectangle: replication 4 (treated) (Esri ArcScene).

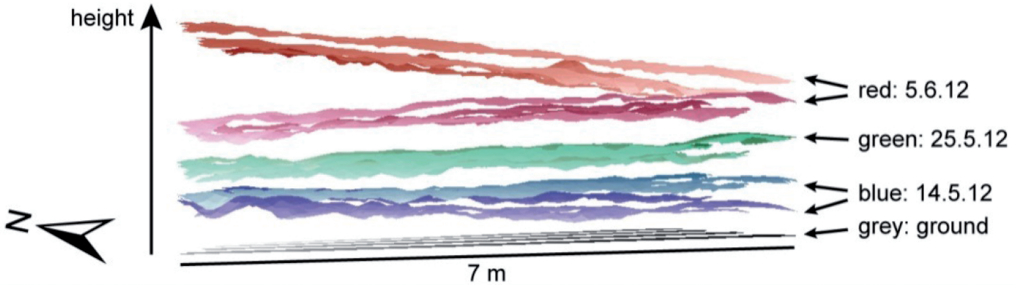

Fig. 6: Cross section of CSM – replication 4 (treated): height comparison (t_0 – t_3) for two datasets of overlapping tiles (t_0 = grey, t_1 = light and dark blue, t_2 = light and dark green, t_3 = light and dark red) (Esri ArcScene, height 2 times exaggerated).

difference 0.02 m. The red surfaces in Fig. 6 of t_3 (5.6.) show maximum differences of 0.36 m and a mean of 0.01 m due to the surface on top increasing in height towards north.

3.3 *Plant Height Development*

The analysis of plant height and the growth according to cultivar and treatment is presented

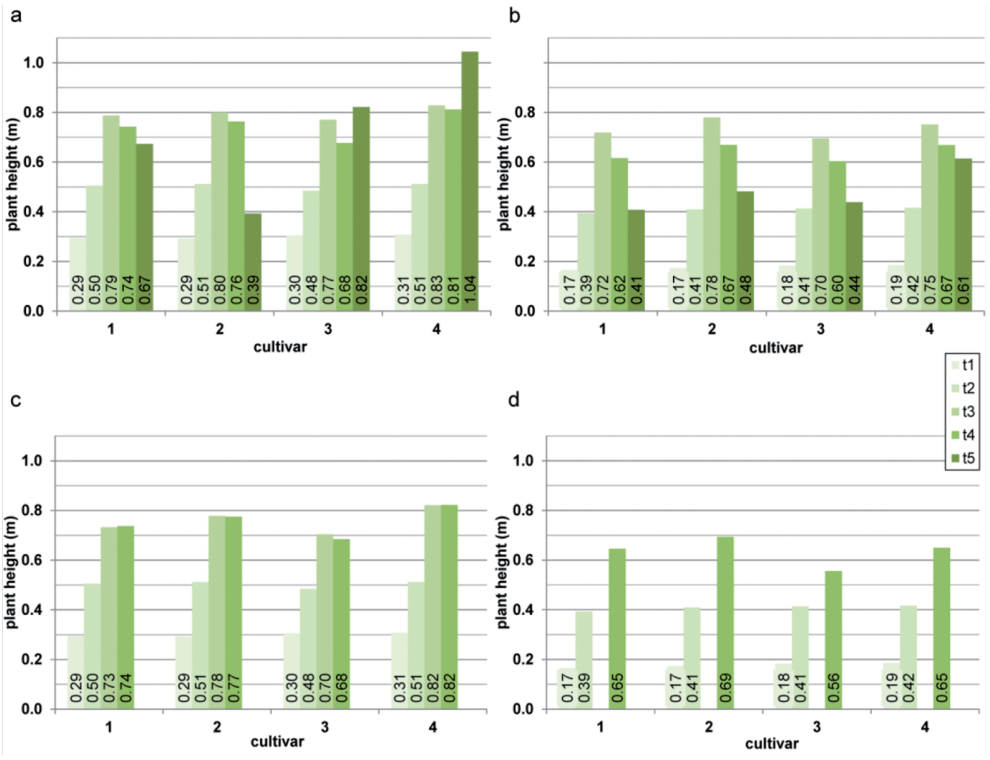

Fig. 7: CSM – mean plant height comparison according to date, cultivar and treatment; a: treated (all data), b: untreated (all data), c: treated (selected data), d: untreated (selected data) (for definition of "selected data" see 2.4.).

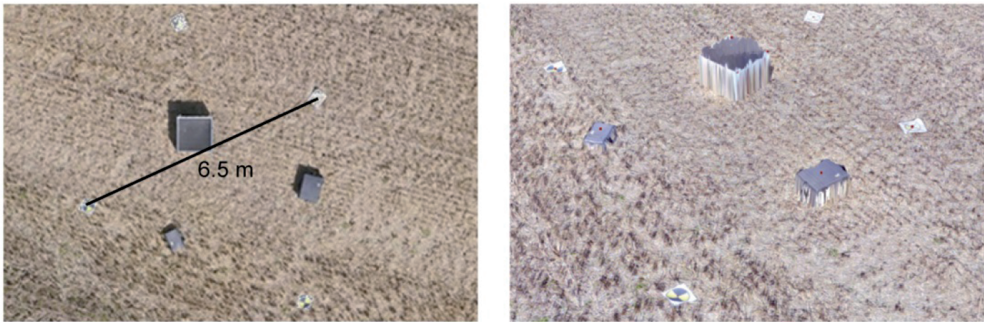

Fig. 8: Experimental design of accuracy assessment (left: photo, right: DEM): Reference points are four GCPs, two different sized Peli Cases and 4 corners of the UAV transport box.

in Tab. 2 and Fig. 7 for all data and selected data (in brackets).

Fig. 7 shows that plants in untreated plots are generally smaller than plants in treated plots. Numbers in Tab. 2 give more details, for example cultivar 1: 0.295 m compared to 0.165 m for t_1 minus t_0. Looking at column t_4 minus t_0, plants in untreated plots are 0.109 m (0.118 m) lower on average (mean height treated: 0.749 m (0.755 m) and untreated: 0.639 m (0.636 m)).

In general, height differences increase between cultivars during the growing season, e. g. orange bars compared to green bars in Fig. 7a or Tab. 2: 0.016 m for t_1 minus t_0 compared to 0.135 m for t_4 minus t_0 for treated plots, all data. Mean heights between cultivars differ by 0.135 m (0.138 m) for treated plots and 0.065 m (0.137 m) respectively for untreated plots (t_4 minus t_0). For t_4 minus t_0 cultivar 3 has the smallest heights while the cultivar with most growth is cultivar 4 for the treated plots and cultivar 2 for the untreated plots (t_4 minus t_0).

3.4 *Accuracy Assessment*

To determine the quality of DEMs generated from stereo images acquired with the UAV-system an accuracy assessment was carried out (Fig. 8). X-, y- and z-coordinates of test targets and four GCPs were measured using DGPS and compared to pixel values in the DEM (flying height 30 m). The test targets were two Peli Cases of different sizes of which each midpoint was measured and the transport box for the UAV (0.75 m x 0.75 m x 0.365 m) of which the four corners were measured. Z-values and differences between DGPS and DEM are presented in Tab 3. Numbers in italic mark differences measured for the four corners of the transport box. The mean height difference is 0.01 m which is in the same order as the accuracy of the DGPS measurement of 0.01 m in z-direction. The differences for the corners of the transport box are above average with 0.02 m which is probably due to the grooved surface of the box. R^2 for the correlation between DGPS and DEM is 0.99.

Tab. 2: Plant height and growths (m) ($t_0 - t_4$) according to cultivar and treatment. Shading in the last column indicates ranking of the amount of growth according to cultivar (dark = big, bright = small) (for definition of "selected data" see 2.4.).

cultivar	date		t_0	t_1-t_0	t_2-t_1	t_2-t_0	t_3-t_2	t_3-t_1	t_3-t_0	t_4-t_3	t_4-t_2	t_4-t_1	t_4-t_0
1	all data	treated	0.000	0.295	0.210	0.505	0.282	0.492	0.787	-0.045	0.237	0.447	0.742
2			0.000	0.293	0.219	0.511	0.289	0.508	0.800	-0.037	0.252	0.471	0.763
3			0.000	0.305	0.179	0.484	0.286	0.465	0.770	-0.093	0.193	0.372	0.677
4			0.000	0.308	0.203	0.511	0.316	0.520	0.828	-0.016	0.300	0.503	0.812
1		untreated	0.000	0.165	0.228	0.393	0.326	0.554	0.719	-0.103	0.222	0.450	0.616
2			0.000	0.173	0.236	0.409	0.370	0.606	0.780	-0.111	0.260	0.496	0.669
3			0.000	0.183	0.230	0.413	0.282	0.512	0.695	-0.092	0.190	0.421	0.604
4			0.000	0.185	0.231	0.416	0.335	0.566	0.751	-0.083	0.252	0.483	0.668
1	selected data	treated	0.000	0.295	0.210	0.505	0.228	0.437	0.732	0.004	0.232	0.442	0.737
2			0.000	0.293	0.219	0.511	0.267	0.485	0.778	-0.003	0.264	0.482	0.775
3			0.000	0.305	0.179	0.484	0.220	0.399	0.704	-0.020	0.200	0.379	0.684
4			0.000	0.308	0.203	0.511	0.309	0.513	0.821	0.001	0.311	0.514	0.822
1		untreated	0.000	0.165	0.228	0.393	no data				0.252	0.480	0.646
2			0.000	0.173	0.236	0.409					0.284	0.520	0.693
3			0.000	0.183	0.230	0.413					0.143	0.373	0.556
4			0.000	0.185	0.231	0.416					0.233	0.464	0.649

Tab. 3: Comparison of heights (m) measured by DGPS and pixel values of DEM for accuracy assessment.

DGPS	DEM	Difference
126.261	126.257004	0.003996
126.151	126.164001	−0.013001
126.181	126.166000	0.015000
126.219	126.224998	−0.005998
126.529	126.504997	0.024003
126.409	126.393997	0.015003
126.713	126.728996	*−0.015996*
126.730	126.704002	*0.025998*
126.734	126.707001	*0.026999*
126.716	126.691002	*0.024998*
	mean	**0.0101002**

4 Discussion and Conclusion

The study area, experiment design and validation results underlined the suitability of stereo images from optical cameras mounted on UAV systems for crop growth monitoring. This enables DEM/CSM generation for agricultural purposes (Hoffmeister et al. 2010). Other campaigns like the ones by Grenzdörffer et al. (2008), Hunt et al. (2010) and Lelong et al. (2008) already mentioned the great potential of UAVs in the field of agriculture.

The MK-Oktokopter by HiSystems GmbH low-cost platform produces competitive results to the often used Microdrone MD4-200, Falcon 8 (Eisenbeiss & Sauerbier 2011) and other UAVs (e. g. Aber et al. 2010, Eisenbeiss et al. 2005, Vallet et al. 2011).

Still some improvements will be made in the future: the UAV-system will be equipped with a camera holder that enables pitch and roll compensation during the flight. This ensures the capture of images in nadir position during movement of the UAV-system. A camera with increased resolution will be used (Panasonic Lumix DMC GX1, 16 mio. pixel) in order to increase ground resolution. It can be triggered electrically which makes image acquisition more reliable compared to a mechanical trigger.

Size, design, texture and number of the GCPs were suitable for the study since they could be clearly identified in the images. With increasing density and height of vegetation the visibility of the GCPs at the chosen placement was obstructed by plants in some cases. To enhance data quality GCPs will be placed in unobstructed positions. The accuracy of the GCPs could be slightly improved by using a total station as Harwin & Lucieer (2012) found out, but would make data collection more time consuming.

Flight planning including flight route generation and data acquisition points enabled capturing images of the whole study area. For t_3, t_4 and t_5 weather conditions during data collection, mainly wind, influenced the quality of the CSMs. Generally weather conditions limit the applicability of a UAV-system for data collection.

The overlap of 50% between the images will be increased in the future in order to cover the study area from numerous positions leading to a greater variety of viewing perspectives. Haala & Rothermel (2012) used 80% overlap, stating that using additional stereo pairs enhances the point clouds, especially in previously occluded areas.Another study by Hartmann et al. (2012) suggest 90% overlap leading to 0.01 m horizontal and 0.03 m vertical accuracy.

Different settings were tested in Agisoft PhotoScan showing that model quality increased with the amount of photos used for

model generation. This is also stated by Roberts et al. (2011). The number of photos taken during the flights will be increased in the future because higher accuracy is expected. The inclusion of photos that were discarded before due to insufficient sharpness, exposure or coverage of the area did not decrease the model quality but on the contrary led to increased model quality in some cases.

Dividing the model of the study area into two tiles led to datasets with manageable data size and provided the opportunity of model comparison. The comparison showed satisfying results for good quality data (e.g. t_2, Fig. 6) with a mean difference of z-values of 0.02 m. An error of this magnitude corresponds to the results of the accuracy assessment which shows a mean error of 0.01 m. Harwin & Lucieer (2012) achieved an accuracy of 0.025 cm – 0.04 cm with a DGPS at a comparable flying height of 40 m – 50 m. Taking other sources of error into account like inaccuracies caused by moving plants during data acquisition or inaccuracy of the DGPS, the resulting CSMs enable plant growth monitoring with very high accuracy.

The comparison of plant heights derived from CSM and infield control surveys showed that for t_4 the range of values is twice as large in the CSM (0.42 m) compared to the infield control survey (0.21 m). This is mainly due to the underestimation of heights in the model especially in the southern part of the field where the untreated plots are located. In this part of the field the range of height values is about 0.06 m larger compared to the northern part of the field. The same is true for the mean height difference between CSM and infield control survey compared to treated plots. Two possible sources of error might account for those differences: The CSMs become more complex with progressing phenology as differences in plant heights increase. This makes modelling difficult as only one viewing perspective (nadir) was chosen and some areas might not have been covered sufficiently. Harwin & Lucieer (2012) suggest data collection from different perspectives. This would further increase the time required for data collection. Continuous acquisition of nadir images using the electrical trigger could address this problem avoiding time consuming measurements.

A second reason is the accuracy of infield control surveys. Determining average plant height is difficult due to high variability of heights in a plot and the fact that plants are moving by wind. A higher number of samples for the control surveys could help to increase accuracy.

Fig. 6 shows that with the method presented in this study it is possible to derive multi-temporal CSMs similar to the concept presented in Fig. 1. The transferability of the concept used for a TLS (Hoffmeister et al. 2010) to a different platform, the UAV, is possible. The partial models show a similar surface profile, if the quality of the raw data is sufficient (problematic are: t_3, t_4 and t_5).

The statistical analysis of the models showed detectable differences between growth according to the cultivar and the treatment. When plants were treated with fungicides, the overall plant height was 15% higher compared to untreated plants. The plant heights of cultivar 3 were 14% lower compared to better growing cultivars 2 and 4.

5 Outlook

In the planned field campaign of 2013, the results obtained from the CSM analysis will be combined with data captured by a multispectral (Tetracam's MiniMCA) and a thermal sensor (NEC F30IS) (Bendig et al. 2012). Thus additional spectral and thermal patterns will be analysed between plant height, which is linked to biomass, vegetation indices, derived from multispectral data (Hunt et al. 2010), and plant temperature (Berni et al. 2009), derived from thermal data. Additionally, the approach will be applied to different crops with varying growth patterns like rice, sugar beet and maize in 2013 in order to investigate the transferability of the concept of multi-temporal CSMs.

Acknowledgements

The authors acknowledge the funding of the CROP.SENSe.net project in the context of Ziel 2-Programms NRW 2007-2013 "Regionale Wettbewerbsfähigkeit und Beschäftigung

(EFRE)" by the Ministry for Innovation, Science and Research (MIWF) of the state North Rhine Westphalia (NRW) and European Union Funds for regional development (EFRE) (005-1103-0018).

In addition, we thank the Institute for Agricultural Plants and Resource Protection (INRES) – Horticultural Science of University of Bonn (Prof. Dr. Georg Noga, Dr. Mauricio Hunsche and Georg Leufen), for providing the experiment field.

We would like to thank Dr. Kai Schmidt and the Julius-Kühn-Institute (JKI), branch office Elsdorf, for providing the test site for the accuracy assessment.

References

Ascos PED, 2010: Der präzise Echtzeitdienst. – http://www.ascos.de/uploads/tx_v3downloads/Produktblatt_PED_2010.pdf (10.1.2013).

Aber, J.S., Marzloff, I. & Ries, J.B., 2010: Small-Format Aerial Photography. Principles, Techniques and Geoscience Applications. – First Edition, 266 p., Elsevier, Amsterdam, The Netherlands.

Agisoft, 2013: http://www.agisoft.ru (8.1.2013).

Bendig, J., Bolten, A. & Bareth, G., 2012: Introducing a low-cost Mini-UAV for thermal- and multispectral-imaging. – International Archives of the Photogrammetry, Remote Sensing and Spatial Information Sciences **XXXIX** (B1): 345–349.

Berni, J.A.J., Zarco-Tejada, P.J., Suárez, L. & Fereres, E., 2009: Thermal and narrowband multispectral remote sensing for vegetation monitoring from an unmanned aerial vehicle. – IEEE Transactions on Geoscience and Remote Sensing **47** (3): 722–738.

De Reu, J., Plets, G., Verhoeven, G., De Smedt, Ph., Bats, M., Cherretté, B., De Maeyer, W., Deconynck, J., Herremans, D., Laloo, P., Van Meirvenne, M. & De Clerq, W., 2013: Towards a three-dimensional cost-effective registration of the archaeological heritage. – Journal of Archaeological Science **40:** 1108–1121.

Eisenbeiss, H., Sauerbier, M., Zhang, L. & Grün A., 2005: Mit dem Modellhelikopter über Pinchango Alto. – Géomatique Suisse **9:** 510–515.

Eisenbeiss, H., 2009: UAV Photogrammetry. – IGP Mitteilungen Nr. 105, Zürich, Schweiz.

Eisenbeiss, H. & Sauerbier, M., 2011: Investigation of UAV systems and flight modes for photogrammetric applications. – The Photogrammetric Record **26** (136): 400–421.

Grenzdörffer, G.J., Engel, A. & Teichert, B., 2008: The photogrammetric potential of low-cost UAVs in forestry and agriculture. – The International Archives of the Photogrammetry, Remote Sensing and Spatial Information Sciences **XXXVII** (B1): 1207–1214.

Haala, N. & Rothermel, M., 2012: Dense Multi-stereo matching for high quality digital elevation models. – PFG – Photogrammetrie, Fernerkundung, Geoinformation **2012** (4): 331–343.

Hansen, P.M. & Schjoerring, J.K., 2003: Reflectance measurement of canopy biomass and nitrogen status in wheat crops using normalized difference vegetation indices and partial least squares regression. – Remote Sensing of Environment **86** (4): 542–553.

Harwin, S. & Lucieer, A., 2012: Assessing the accuracy of georeferenced point clouds produced via multi-view stereopsis from Unmanned Aerial Vehicle (UAV) imagery. – Remote Sensing **4:** 1573–1599.

Hartmann, W., Tilch, S., Eisenbeiss, H. & Schindler, K., 2012: Determination of the UAV position by automatic processing of thermal images. – International Archives of the Photogrammetry, Remote Sensing and Spatial Information Sciences **XXXIX** (B6): 111–116.

HiSystems GmbH, 2013: http://www.hisystems.de (8.1.2013).

Hoffmeister, D., Bolten, A., Curdt, C., Waldhoff, G. & Bareth, G., 2010: High resolution Crop Surface Models (CSM) and Crop Volume Models (CVM) on field level by terrestrial laserscanning. – SPIE Proceedings **7840**.

Hunt, E.R., Hively, W.D., Fujikawa, S.J., Linden, D.S., Daughtry, C.S.T. & McCarty, G.W., 2010: Acquisition of NIR-green-blue digital photographs from unmanned aircraft for crop monitoring. – Remote Sensing **2:** 290–305.

Lelong, C.C.D., Burger, P., Jubelin, G., Roux, B., Labbé, S. & Baret, F., 2008: Assessment of unmanned aerial vehicles imagery for quantitative monitoring of wheat crop in small plots. – Sensors **8:** 3557–3585.

Mikrokopter, 2013a: NaviCtrl V2.0. – http://www.mikrokopter.de/ucwiki/NaviCtrl_2.0 (8.1.2013).

Mikrokopter, 2013b: MikroKopterTool-OSD. – http://www.mikrokopter.de/ucwiki/mikrokoptertool-osd (8.1.2013).

Mulla, D.J., 2012: Twenty five years of remote sensing in precision agriculture: Key advances and remaining knowledge gaps. – Biosystems Engineering **XXX:** 1–14.

Neitzel, F. & Klonowski, J., 2011: Mobile 3D mapping with a low-cost UAV system. – International Archives of the Photogrammetry, Remote

Sensing and Spatial Information Sciences **XXXVIII-1** (C22): 1–6.

Panasonic, 2013: http://94.23.55.209/index.php/Cameras/Camera-Sensor-Database/Panasonic/Lumix-DMC-GF3 (8.1.2013).

Perko, R., Raggam, H., Gutjahr, K. & Schardt, M., 2010: Analysis of 3D Forest Canopy Height Models Resulting from Stereo-Radargrammetric Processing of TerraSAR-X Images. – Remote Sensing for Science, Education, and Natural and Cultural Heritage: 537–545.

Roberts, R., Sinha, S.N., Szeliski, R. & Steedly, D., 2011: Structure from motion for scenes with large duplicate structures. – IEEE Computer Society Conference on Computer Vision and Pattern Recognition: 3137–3144.

St-Onge, B., Vega, C., Fournier, R.A. & Hu, Y., 2008: Mapping canopy height using a combination of digital stereo-photogrammetry and lidar. – International Journal of Remote Sensing **29** (11): 3343–3364.

Szeliski, R., 2010: Computer Vision: Algorithms and Applications. – First Edition, 812 p., Springer, London, UK.

Thenkabail, P.S., Smith, R.B. & Pauw, E.D., 2000: Hyperspectral vegetation indices and their relationship with agricultural crop characteristics. – Remote Sensing of Environment **71** (2): 152–182.

Vallet, J., Panissod, F., Strecha, C. & Tracol, M., 2011: Photogrammetric performance of an ultra light weight swinglet "UAV". – International Archives of the Photogrammetry, Remote Sensing and Spatial Information Sciences **XXXVIII-1** (C22): 1–6.

Verhoeven, G., 2011: Taking computer vision aloft – Archaeological three-dimensional reconstructions from aerial photographs with PhotoScan. – Archaeological Prospection **18:** 67–73.

Verhoeven, G., Doneus, M., Briese, Ch. & Vermeulen, F., 2012: Mapping by matching: a computer vision-based approach to fast and accurate georeferencing of archaeological aerial photographs. – Journal of Archaeological Science **39:** 2060–2070.

Address of the Authors:

Juliane Bendig, Dr. Andreas Bolten, Prof. Dr. Georg Bareth, Institute of Geography, GIS & RS Group, University of Cologne, Albertus-Magnus-Platz, D-50923 Köln, Tel.: +49-221-470-6265, Fax: +49-221-470-8838, e-mail: {juliane.bendig}{andreas.bolten}{g.bareth}@uni-koeln.de

Manuskript eingereicht: Februar 2013
Angenommen: Juni 2013